
MODELING THE FATE OF TOLUENE IN A CHAMBER WITH ALFALFA PLANTS

2. NUMERICAL RESULTS AND COMPARISON STUDY

M. Narayanan¹, J.C. Tracy², L.C. Davis³, and L.E. Erickson¹

Department of Chemical Engineering¹ and Biochemistry³, Kansas State University, Manhattan, KS 66506; Water Resources Center, Desert Research Institute², Reno, NV 89506

ABSTRACT

Investigations were conducted in a chamber to study the role of alfalfa plants in bioremediating toluene. Modeling and experimental results indicate that *in situ* bioremediation of toluene in the presence of plants is feasible and economical. This is primarily due to evapotranspiration which greatly enhances the vertical transport of dissolved contaminants from the saturated zone to the rhizosphere, thereby increasing the possibility of aerobic degradation. The fate of toluene was simulated and monitored for groundwater contaminated with toluene at saturated concentrations. FT-IR instrumentation was used to monitor toluene in the headspace gas of the vegetated chamber. Overall mass balance, based on groundwater and headspace measurements, indicated about 75% loss or biodegradation of toluene from the chamber during steady state. Evolution of significant amounts of CO₂ accounted for mineralization of toluene. Simulation results predicted toluene biodegradation in the unsaturated zone where both oxygen and toluene were present. Dispersion processes in the soil were characterized by bromide tracer analysis. Predictions from simulations were compared with the water content and toluene concentrations measured in the chamber.

Key words: *biodegradation, toluene, gas phase diffusion, phytoremediation, soil, alfalfa*

INTRODUCTION

Toluene is present in most sites contaminated with gasoline and related mixtures of petroleum hydrocarbons. Leaking underground storage tanks and transporting pipelines are widespread sources for toluene, a volatile organic chemical (VOC) which is classified by the U.S. EPA as a hazardous organic pollutant. In addition to contaminating groundwater, VOCs may also partition into the gas phase and be released into the atmosphere. Studies have indicated that bioremediation is an effective technology in terms of economics, labor, and liability in remediating sites contaminated with toluene (Borden et al., 1986; Lee et al., 1988). Under aerobic conditions, biodegradation of toluene in soils is usually rapid.

Several reviews on the degradation of toluene under controlled environments describe the formation of intermediate products (Gibson and Subramanian, 1984). Biodegradation by indigenous soil microbes of toluene in a BTEX mixture was demonstrated in laboratory experiments under aerobic, denitrifying, iron-reducing, sulphate-reducing, and methanogenic conditions (Chen et al., 1992). Recently, Jin et al. (1994) investigated the effect of microbial degradation on toluene transport through an unsaturated soil column under varying soil conditions and toluene feed concentrations. They reported that acclimatization of indigenous microbes greatly enhances toluene degradation and under such conditions a 30 cm soil cover over a toluene source could prevent the volatilization of toluene to the atmosphere. In their study, they were interested in biodegradation of toluene introduced in the unsaturated zone. In the laboratory, Alvarez et al. (1994) studied toluene degradation by denitrifying aquifer microorganisms in order to extend results to *in situ* enhanced bioremediation schemes. They observed that

toluene degradation by denitrifying bacteria was adequately characterized by the Monod equation. Successful clean up of toluene in BTEX-contaminated aquifers has also been reported (Lee et al., 1988; Chiang et al., 1989).

The design and utilization of plant-based bioremediation (phytoremediation technology) of a site contaminated with organic compounds has many promising features. Investigations by several researchers show that vegetation plays a key role in enhancing the biodegradation of many organic pollutants (McFarlane et al., 1981; Walton and Anderson, 1990; Anderson et al., 1993; Cunningham and Berti, 1993; Shimp et al., 1993; Erickson et al., 1994; Ferro et al., 1994; Gatliff, 1994; Narayanan et al., 1995a; Narayanan et al., 1995b; Schnoor et al., 1995; Davis et al., 1998).

The review by Davis et al. (1998) describes the role of vegetation in the phytoremediation strategies which are currently employed. Moderately hydrophobic compounds such as BTEX, agricultural chemicals such as atrazine, excess nutrients such as nitrates and phosphates, ammunition compounds, and many other organic contaminants present in soil and groundwater have been effectively biodegraded. Vegetative mediated remediation is suited for unconfined aquifer systems with contamination at depths shallower than 30 feet (Gatliff, 1994; Schnoor et al., 1995; Davis et al., 1998). Vegetation may also control the infiltration of landfill leachates and movement of dissolved contaminants into groundwater aquifers (Licht, 1993).

Biodegradation of organics occurs in the rhizosphere (root zone of the plants) (McFarlane et al., 1981; Walton and Anderson, 1990; Anderson et al., 1993; Cunningham and Berti, 1993; Shimp et al., 1993; Erickson et al., 1994; Ferro et al., 1994; Narayanan et al., 1995a; Schnoor et al., 1995; Davis et al., 1998). Plant roots exude a wide spectrum of compounds from sugars, amino acids, and carbohydrates to essential vitamins which may act as growth and energy substrates for the microbes. Earlier studies showed that the rhizosphere can either act as a natural sink for the depletion of atmospheric benzene vapors (McFarlane et al., 1981) or enhance biodegradation of trichloroethylene (Walton and Anderson, 1990; Narayanan et al., 1995b) and degradation of pentachlorophenol by as much as threefold in crested wheat grass soil (Ferro et al., 1994).

In the process of bioremediation, vegetation may take up, translocate or immobilize, and transform the organics. The most important parameter to predict plant uptake from the soil is its octanol-water partition coefficient, K_{ow} (usually, expressed as $\log K_{ow}$) (Cunningham and Berti, 1993). For barley plants, Briggs et al. (1982) studied the uptake of non-volatile compounds in homologous series but with varied octanol-water partition coefficients. They found that non-volatile pesticide compounds with partition coefficient values of about 100 ($\log K_{ow} = 2$) show a maximum translocation into the transpiration stream of the plant; typically this is as much as 80% of soil-water contaminant concentration. They also cited examples of compounds that deviate from the predictive transpiration stream concentration curve. Compounds with low $\log K_{ow}$ values (≤ 1) are relatively mobile in both the plant xylem and phloem. Compounds with $\log K_{ow}$ values between 1 and 4 are generally considered to be

xylem mobile and phloem immobile. Compounds with high $\log K_{ow}$ values (³⁴) are generally not substantially translocated into the plants. Additionally, accumulation of organics, resulting from uptake and immobilization, could also be phytotoxic. Researchers are extending the degrading capacity of soil microflora to plants by incorporating microbial genes into the plant genomes to tackle this problem (Stomp et al., 1994). Trapp and McFarlane (1995) discuss in much greater detail a wide range of contaminants and their interaction with plants.

Evapotranspiration associated with photosynthesis helps plants to draw water up into the vadose zone. This solar-driven pumping increases the net upward flux of water through the vadose zone, thus lowering the groundwater table and decreasing the soil-water content. This results in increased oxygen transfer by gas-phase diffusion in the soil. More importantly, evapotranspiration also brings dissolved organics to the rhizosphere soil for biodegradation by the microbial consortia which are supplied with basic nutrients from the plants. The solar-driven pumping may translocate organic pollutants into plants, depending on their volatility and $\log K_{ow}$.

The plant root system may also act as a pathway for the diffusion of oxygen to the rhizosphere microflora (Shimp et al., 1993; Davis et al., 1998). Under aerobic conditions, the microbial consortia may biodegrade the organics before they can be taken up and translocated into the plant. In summary, the plant and associated rhizosphere act as an active and relatively favorable *in situ* bioreactor for the growth of microbes and transformation of contaminants in two essential ways:

- (a) Continuously supplying basic nutrients such as C, N, and P for microbial growth because of fixation and exudation processes; and
- (b) Enabling higher diffusivity of atmospheric oxygen into the soil as a result of the removal of water by the evapotranspiration process.

The objective of this part of the work was to compare the results from laboratory experiments performed in order to study the fate of toluene in presence of alfalfa plants with that of the modeling results. Simulation results were obtained by employing a two-dimensional model. The model was originally developed in three dimensions but was implemented in two dimensions for comparison with experimental results (Narayanan et al., 1998). The detailed description of the experimental setup and data collection from the experiments performed are described in Narayanan (1994).

EXPERIMENTAL STUDY

A chamber with two identical U-shaped channels each 10 cm wide, approximately 1.8 m in axial flow length, and 35 cm in depth was employed (Figs. 1 and 2). The design and construction of this chamber were described in Narayanan (1994). Silty sand soil (silt < 10%) collected from 3 zones along the depth from near a landfill were packed in the channels. The description of the soil and packing were described by Narayanan (1994). Alfalfa plant growth began with feeding toluene contaminated water to the channel under laboratory conditions. Toluene was fed at saturated concentrations of 550 mg/L at

26°C for 11 months. Four groundwater monitoring wells, installed along the axial flow length of the channels, facilitated frequent monitoring of compound concentration in the saturated zone (Narayanan et al., 1995a). Figure 2 shows the overhead view of the chamber with alfalfa plants, sampling ports, inlets, and outlets. Figure 1 shows the frontal view of the chamber when it is imagined to be axially extended.

Alfalfa plants received continuous light energy from eight Cool-white fluorescent lamps positioned 40 cm above the soil surface in the chamber. The luminous intensity measured near the soil surface indicated a value of 5-7 klx. However, a 24-hour averaged daily luminous intensity received on a clear summer day is about 30 klx. A glass and aluminum enclosure 26 cm high was constructed above the ground level to measure the headspace gas concentration. A small fan facilitated air mixing in the enclosure. Water vapor condensed onto four refrigeration tubes in which coolant was circulating. Headspace gas of the enclosed chamber was measured using a MIDAC Fourier Transform Infra Red (FT-IR) instrument to detect toluene that was either evaporated through the soil pathway or transpired through the plant pathway (Narayanan et al., 1995a). Carbon dioxide evolution into the headspace from the rhizosphere soils was also measured using the FT-IR spectrophotometer (Narayanan et al., 1995a). The adsorption characteristics of toluene were analyzed by making a step change in the inflow groundwater concentration from water saturated with toluene to pure distilled water. The concentration of toluene in the groundwater was measured regularly until the transient response was completed.

Tracer Experiment

To study the dispersion characteristics and movement of groundwater due to evapotranspiration associated with vegetation, bromide tracer studies were conducted. Six liters of KBr solution were fed at a concentration of 150 mg of KBr/L. The bromide tracer was input as a broad pulse for a period of 203 hours. The concentration of bromide in the groundwater samples collected from sampling wells was measured using an ion chromatograph.

Contaminant degradation

During the steady state operation of the experiment, the concentration of toluene at various port locations remained approximately uniform along the length of the channel and constant over the steady state period of operation. In other words, spatial (along the axial length) and temporal variations in toluene concentration were minimal. Fourier Transform Infra Red (FT-IR) headspace measurements of the chamber showed that gas phase concentrations of toluene were below the detection limit of the instrument of about 1 ppm (v/v). The results are already described in Narayanan et al. (1995a).

The indigenous, well-adapted, and mixed microbial consortia in the vadose zone contributed to the loss of toluene that was transported in the vertical direction. Carbon dioxide evolution into the headspace of the chamber suggested that about 50% of the inflow carbon was evolved as CO₂ due to aerobic biodegradation. Biodegradation was also reported in another independent study by Jin et al. (1994). They observed that toluene was completely mineralized in the soil column with indigenous

microorganisms previously acclimated to toluene vapors. We have also repeated treatments with toluene at 100 mL/L input in presence of trichloroethylene (TCE) at 10 mL/L or 100 mL/L and confirmed complete disappearance of toluene but not TCE at a depth of 10-15 cm below the surface of the soil.

Water Content

During steady state operation, soil samples were collected from different locations and at different depths from each location along the channel to measure the gravimetric water content. The measurements indicated that the degree of saturation varied from about 70% near the surface (corresponding to a volumetric water content, $\alpha_v = 0.27$) to about 99% near the groundwater table ($\alpha_v = 0.35$) (Narayanan et al., 1995a) where the value of α_v approaches the porosity of the soil.

SIMULATING PHYSICAL CONDITIONS

As described in the previous section, the model parameters representing the physical conditions within the experimental chamber and the influx of toluene are not expected to vary significantly across the width of the chamber. Thus, the modeling domain can be simulated in two dimensions, these being the vertical and the longitudinal flow directions. The channel was modeled as a two-dimensional spatial grid with a network of 400 elements and 441 nodes. One of the dimensions for simulation was the longitudinal direction, x , while the other dimension was the vertical direction, z . The 1.8 m long and 35 cm deep channel was discretized and subdivided into several regions. A schematic of this network of partitioned regions is shown in Figure 3. Elements belonging to a particular region had the same size and area. Region A had elements of size 5.5 cm X 2 cm, region B had elements of size 5.5 cm X 1 cm, region C had elements of size 11 cm X 1 cm, region D had elements of size 12 cm X 1 cm, region E had elements of size 11 cm X 2 cm, and region F had elements of size 12 cm X 2 cm (Figure 3). This kind of partitioning was adopted in order to capture the sharp discontinuities in the concentration profiles of solutes at the inlet boundary ($x = 0$ and $z = 0-5$ cm), soil surface (all x and $z = 35$ cm), and outlet boundary ($x = 180$ cm and $z = 0-5$ cm). The largest and smallest element of this hypothetical network of elements had areas of 24 and 5.5 cm², respectively.

In Narayanan et al. (1998), Eqs. (1), (2), and (34)-(37) were a set of six coupled non-linear partial differential equations in three dimensions. However, for comparison of numerical results with experimental study, the three-dimensional model was implemented in only two dimensions. Then, the six equations have 3 independent variables, t to represent temporal changes, and x, z to represent two dimensional spatial variations. The six principal dependent variables that are simulated using the Eqs. (1), (2), and (34)-(37) are $C_s, C_b, C_o, C_r, Y_s,$ and Y_r (Narayanan et al., 1998). All other dependent variables such as $\alpha, K_s, V_r, D_{ij}, x,$ and m are either explicitly or implicitly related to the six principal variables through constitutive mathematical relationships described in Narayanan et al. (1998).

Initial and Boundary Conditions

The initial conditions (ICs) and boundary conditions (BCs) were developed based on the physical setup of the laboratory chamber. The ICs at time $t = 0$ and all x, z for Eqs. (34)-(37) were assumed for some cases as:

$$C_s = 500 \text{ mg/L}; \quad C_b = 0.01 \text{ mg/L}; \quad C_r = 2 \text{ mg/L}; \quad C_o = 1 \text{ mg/L}.$$

However, in some simulations the initial conditions for Eqs. (1), (2), and (34)-(37) were obtained by initially assuming a steady state condition for the first time step of the simulation (Narayanan et al., 1998). This condition was essentially obtained by setting the left hand side of Eqs. (1), (2), and (34)-(37) to zero (Narayanan et al., 1998). The unknowns were then computed for all 441 nodes. These values were then used as initial conditions for the following time steps of the simulation. After the first time interval, subsequent computations were carried out in an unsteady state manner as given by Eqs. (1), (2), and (34)-(37) (Narayanan et al., 1998).

For the boundary conditions at the inlet, $x = 0$ and $z = 5$ cm (Fig. 2), the inflow conditions were assumed as distributed influx boundary conditions. The inflow rate was assumed to be distributed on a boundary represented by $x = 0$ and $z = 0-5$ cm in the experimental chamber. This assumption was made to avoid any complexities introduced into the simulation by imposing a point source to the domain. Hence, at the inlet boundary while simulating the soil-water flow Eq. (1), the daily recorded water inflow rate to the channel was assumed as a distributed influx to the system at the inlet boundary ($x = 0$ and $z = 0-5$ cm). For simulating species transport Eqs. (34)-(37) (Narayanan et al., 1998) during contaminant feeding operation, the following boundary conditions were used at the inlet boundary: $C_s = 550$ mg/L, $C_b = 0$, $C_o = 8$ mg/L, and $C_r = 0$. However, during pure water feeding operation, in order to study sorption characteristics, the following boundary conditions were used at the inlet boundary: $C_s = 0$, $C_b = 0$, $C_o = 8$ mg/L, and $C_r = 0$. The inlet oxygen concentration C_o was 8 mg/L during all feeding operations because the input feed water is always saturated with dissolved oxygen. This may be compared to a situation where the subsurface groundwater is replenished by recharging with water at saturated concentrations of dissolved oxygen (8 mg/L).

A similar distributed outflux assumption was made at the outlet, $x = 180$ cm and $z = 5$ cm. Outflow was assumed to be distributed on a boundary represented by $x = 180$ cm and $z = 0-5$ cm of the chamber. For simulating the water outflow from the outlet boundary, a constant head boundary condition was used in the model. The total soil-water pressure head was set at 0.05 m at the outlet boundary ($x = 180$ and $z = 0-5$ cm). In transport equations (34)-(37), the gradient in concentration was assumed to be zero at the outlet boundary ($x = 180$ cm and $z = 0-5$ cm).

$$\frac{\partial C_s}{\partial x} = \frac{\partial C_r}{\partial x} = \frac{\partial C_b}{\partial x} = \frac{\partial C_o}{\partial x} = 0$$

For soil and root-water flow Eqs. (1) and (2) (Narayanan et al., 1998), boundary conditions at the surface were the outflux of water from the soil surface based on the total observed evapotranspiration (*ET*). The total observed evapotranspiration rate was used to calculate the potential evaporation (Eq. (13) (Narayanan et al., 1998)) and transpiration rates (Eq. (18) (Narayanan et al., 1998)) from the vegetated system. For solute transport according to Eqs. (34)-(37) (Narayanan et al., 1998), at the soil surface, the following assumptions were made. Oxygen from the atmosphere was assumed to diffuse into the chamber through the gas and aqueous phases. In other words, the oxygen concentration of soil-water at the surface was assumed to be saturated with oxygen because of rapid partitioning of atmospheric O₂ into surface soil-water. The contaminant concentration was assumed to be zero at the soil surface. This was done in order to be consistent with the experimental observations reported by Narayanan et al. (1995a). Concentrations of microbial biomass and root exudates were assumed to be a no flux or impermeable boundary condition at the soil surface. In the finite element procedure, the no flux boundary condition is assumed to occur when no alternate boundary condition is specified. In other words, an impermeable boundary condition is used at the following boundaries: for all x and $z = 0$, for $x = 0$ and $z = 5-35$ cm, and for $x = 180$ cm and $z = 5-35$ cm.

MODEL EXECUTION AND AVAILABILITY

The simulation runs of the model were mostly performed in a SUN SPARCstation-20 or SUN SPARCstation-10. The execution speed of the model depended on a number of factors other than the computer resources itself. The execution speed was determined by the number of finite elements used to represent the domain, the time step of simulation, and the final time of simulation. For the modeling configuration shown in Figure 3, it was observed that a computer simulation of bromide tracer transport through the channel for about 40 days at a time step of 4 hours consumed about 10 minutes in the above mentioned SUN SPARCstations. However, execution of the same simulation on a 486DX2-66MHz personal computer consumed about 35 minutes of computer time. Similarly, a computer simulation of toluene transport through the channel for about 85 days at a time step of 4 hours consumed about 50 minutes of computer time in the SUN SPARCstations, while simulation runs on a 486DX2-66MHz personal computer consumed about 4 hours. It must be emphasized that when time step was decreased for toluene simulations from 4 hours to 0.1 hours, the time taken on SUN SPARCstations dramatically increased from 50 minutes to 5 hours. The model named as BIOROOT is currently being made user friendly and will be available for contaminated site predictions upon written request to authors when this work is completed.

RESULTS AND DISCUSSION

Soil and root characteristic parameters

Tables 1 and 2 show the values of the various soil and plant characteristic parameters used for the simulation study. The silty sand soil was assumed to have a saturated hydraulic conductivity (K_{sat}) of 0.38 m/hr and porosity (n) of 0.35. Bulk density of soil was measured to be 1.5 g/cm³. These values are typically used for sandy soil (Feddes et al., 1975; Tracy and Marino, 1989; Chen et al., 1992). The soil characteristic parameters, $A = 0.5$ m, $c = 0.9$, and $d = 3.5$, used in Eqs. (4) and (5) (Narayanan et al., 1998), were based on experimentally obtained water content values in the laboratory chamber (Narayanan et al., 1995a). Winter (1983) discussed in detail the influence of parameters A , c , and d on the shapes of the profiles of effective water saturation (S_e) versus soil-water pressure head (y_s), and hydraulic conductivity (K_s) versus effective water saturation (S_e). The plant characteristic parameters, such as K_r and G used in simulation were obtained from previous results from either field or laboratory experiments (Marino and Tracy, 1988; Tracy and Marino, 1989).

Bromide tracer simulation study

A bromide tracer was introduced into the toluene-fed channel in order to study its longitudinal and axial dispersion characteristics and soil-water movement under the influence of evapotranspiration associated with vegetation. The movement of the tracer was modeled as a conservative solute flowing in the groundwater of the chamber with transpiring alfalfa plants. The soil components such as biomass, root exudates, and oxygen transport represented by Eqs. (35)-(37) (Narayanan et al., 1998) were assumed to remain unaffected during bromide tracer studies. To model the bromide tracer transport in the channel, Eq. (34) (Narayanan et al., 1998) was modified to account for convective-dispersive transport of the tracer in presence of transpiring alfalfa plants. Equation (34) may then be written as shown below with all symbols retaining their same meanings.

$$\frac{\partial}{\partial t} [C_k(\theta)] = \frac{\partial}{\partial x_i} \left[\theta D_{ij} \frac{\partial}{\partial x_j} (C_k) - V_i C_k \right] \quad i, j = 1, 2 \quad (53)$$

V_1 (or V_x) and V_2 (or V_z) represent the advective fluxes of water in the soil and are determined using Darcy's law (Eq. 7 (Narayanan et al., 1998)). The soil-water pressure head distribution in Darcy's law is evaluated using Eqs. (1) and (2) (Narayanan et al., 1998). Modeling of the tracer transport was then performed using the three equations (Eqs. (1), (2), and (53)) simultaneously with initial and boundary conditions described earlier. The measured inlet feed water flow rate and measured inlet concentration of bromide were used as inlet boundary conditions at $x = 0$, and $z = 0-5$ cm.

Figures 4-6 show the comparison between the experimental and modeling studies for bromide tracer at ports 1 and 2, 3 and 4, and outlet, respectively. A good comparison between the experimental and simulated curves was obtained; however, the predicted bromide concentration is less than the

measured values from 200-400 hours in Figure 6. The early sharp discontinuity in the curves was due to plugging at the channel inlet in the beginning part of the tracer experiment. This discontinuity feature was also taken into account during the modeling studies. It was observed in tracer simulation that the dispersion coefficients in the soil substantially affected the simulated bromide profiles. Dispersion coefficients are related to the longitudinal dispersivity (α_L) and transverse dispersivity (α_T) according to Eq. (27) (Narayanan et al., 1998). Results were particularly sensitive to values of these dispersivities. Table 1 shows the values of α_L and α_T used for simulation. These were comparable to values used in literature (Chiang et al., 1989; Tracy and Marino, 1989; Chen et al., 1992). However, these values also depend on the smallest size of element used in simulation. Increasing dispersivity results in greater mixing in the system. A large value causes a poor fit of modeled bromide tracer profile to the experimentally observed results near the outlet. In field experiments, a single dispersivity value to account for dispersion in the entire field may not be suitable. Using very low values of dispersivities usually caused instability in the numerical results.

During the experimental study it was found that evapotranspiration significantly influenced the flow rate through the channel. In reality, one would expect that when evapotranspiration rates are sufficiently high, there may be no net outflow from the system and the tracer would take a very long time to arrive at the outlet. Arrival times at the ports are likewise influenced by the evapotranspiration rates associated with the different sections of the channel. Arrival time at any port depends on both distance and net flow, which is dependent on evapotranspiration rate over that distance. Limitations in precise estimation of the relative evapotranspiration rates caused by different plants along different sections of the channel may have also contributed to the slight differences in the comparison of the tracer results.

Figures 7-11 show the contour plots of tracer distribution in the channel at times of 101, 203, 301, 501 and 912 hours of operation. Note that zero, 203, and 912 hours represent the start, step change from tracer to pure water, and end of the tracer experiment. Since bromide does not adsorb to the soil, all of the bromide is in the aqueous phase in these results. It is evident from Figures 7-11 that vertical movement of tracer from saturated zone towards the unsaturated zone is primarily because of evapotranspiration. It can be seen from Figure 11 that an appreciable amount of tracer accumulation is predicted near the surface. This also substantiates the influence of evapotranspiration in the transport of solutes from the saturated zone to the rhizosphere. Soil samples were collected from various locations in the channel along different depths. Bromide concentration measurements in these soil samples were below the detection limits of the ion chromatograph instrument. Therefore, it was not possible to compare bromide concentration along the vertical direction of the channel. It is possible that bromide could be taken up by alfalfa plants during the experiment; however, the concentration of bromide would be less than 10 mg/kg of soil if it was distributed uniformly throughout the chamber.

Plants may actively transpire water by drawing up large quantities of groundwater from the saturated zone. Consequently, accumulations of relatively non-volatile solutes may occur in the surface

soils. This result implies that dissolved contaminants associated with groundwater may also be drawn up to the rhizosphere as part of the phytoremediation strategy. Therefore, evapotranspiration should enhance the contaminant availability to the indigenous microbes present in the rhizosphere. This subsequently enhances the bioremediation process to a great extent. Moreover, in relatively less humid states, like Kansas, where evapotranspiration usually exceeds the overall annual precipitation, phytoremediation strategies could be very effective by efficiently managing a plant ecosystem.

Contaminant fate simulation results

Equations (34)-(37) (Narayanan et al., 1998) were used to model the fate of the contaminants in the rhizosphere. Parameter values used in modeling toluene degradation in the rhizosphere are shown in Table 3. The simulation study involved adjusting the kinetic parameters in the model in order to obtain reasonable comparison between experimental and simulated data. The parameters adjusted were maximum specific growth rate, endogenous decay rates, and Monod saturation constant for toluene and oxygen. The values listed in Table 3 for these parameters are quite comparable to values found in literature (Chiang et al., 1989; Chen et al., 1992). The developed model considers only the aerobic degradation of contaminants in the rhizosphere (Narayanan et al., 1998). Figures 12-15 show the contour plots for distribution of water content, toluene, biomass, and oxygen in the channel during steady state. Figure 12 shows the volumetric water content distribution during this period of operation. The soil-water content in the vadose zone of the shallow system was observed to be relatively high (Narayanan et al., 1995a). The water content variation along the axial length of the channel was insignificant as compared to variation in the vertical direction. The volumetric water content varied from 0.35 (100% of effective saturation) at the bottom to 0.27 (73% of effective saturation) at the top. This was in good agreement with experimentally measured water content values (Narayanan et al., 1995a). These relatively high saturation values are expected in a shallow system with actively transpiring plants. Usually, the capillary zone extends to about 10-15 cm above the groundwater table for fine sandy soil.

Figure 13 reveals the steady state simulated concentration profiles for toluene at various depths of the channel. The simulated toluene concentration remained approximately constant along the axial length at the bottom of the channel during the simulation. This is consistent with the experimental data presented earlier (Narayanan et al., 1995a). The simulated toluene concentration progressively decreased from the bottom to the top of the channel where it approached a concentration of 0 ppm. This was again consistent with the FT-IR measurements of the headspace of the enclosed chamber. It is therefore clear that toluene movement was significantly influenced by evapotranspiration and toluene disappeared in the vadose zone. This disappearance was primarily attributed to the aerobic microbial degradation of toluene in the vadose zone. This is supportive of results from studies performed by Jin et al. (1994).

Figure 14 shows that biomass accumulation was high near the inlet of the channel because of the

availability of dissolved oxygen and toluene in the inflow groundwater. Based on simple assumptions, 10 mg/L biomass concentration represented a cell count of the order of 10^8 cells/g dry weight of soil.

Figure 15 reveals that the oxygen concentration was close to the saturated concentration near the inlet of the channel. The oxygen concentration declined rapidly within 20 cm of the inlet. The oxygen concentration is high immediately below the upper surface due to diffusion of atmospheric oxygen into the gas phase of the channel soil. However, in the simulation, atmospheric oxygen is also depleted rapidly within the top 5 cm of the channel soil. The dissolved oxygen was predicted to be near zero in a large portion of the channel. Anaerobic conditions may therefore be present in the saturated zone away from the inlet.

Parameter sensitivity

Comparison to the observed spatial and temporal variation in tracer and contaminant concentrations were used to calibrate the model. It is important to emphasize that the calibrated parameters are in no way unique. However, the model does predict the contaminant transport, biomass growth, and oxygen consumption for the employed set of model parameters. Specific parameter values were varied to explore their influence on the predicted concentration profiles. These analyses provided information on the sensitivity of the model to the specific parameters and may be useful to predict the outcome of phytoremediation applications to practical sites. The maximum specific growth rate of the biomass, and Monod saturation constants and gas phase diffusivities of toluene and oxygen were among the parameters tested to study the sensitivity of the model.

The Monod saturation constants for toluene and oxygen, which are given in Table 3, were found to have large effects on the simulated curves. Increasing or decreasing the saturation constant by ten-fold gives a distinctly poorer fit with the observed data. The maximum specific growth rate of the biomass also had an appreciable effect on the simulation. This was also reported in earlier studies by Essaid et al. (1995) and Chen et al. (1992). A 10% increase or decrease in maximum specific growth rate of biomass, from 0.1 /hr, significantly affected the steady state concentration of toluene in the channel. It was also observed that when the simulation was run with a zero maximum specific growth rate for the microorganisms, the system became completely saturated with toluene from the bottom to the surface. Death rate constants of microbes, k_{d1} and k_{d2} , were set to 0.01/hr and 0.01 $\text{m}^3/(\text{g}\cdot\text{hr})$. These numerical values were essentially 0.1 times the maximum specific growth. An increase in these constants decreased the accumulation of the biomass concentration levels as expected.

From Figures 13-15 we can see that aerobic biodegradation occurs at a rapid rate as long as oxygen and the contaminant are both present. Oxygen is transported downward while the toluene is transported upward; attenuation occurs where both are present. In locations where the concentration of oxygen in the system was close to zero, biomass concentrations were small, and contaminant concentration remained relatively unchanged. This is clearly reflected in the groundwater away from the entrance zone with biomass and oxygen concentrations close to zero in Figures 14 and 15. This confirms the

findings of earlier studies that suggest that aerobic degradation will occur rapidly and can often be treated as occurring instantaneously (Borden et al., 1986; Rifai et al., 1988; Essaid et al., 1995).

Effective gas-phase diffusivity of toluene was simulated using the Millington-Quirk equation, Eq. (26), based on the gas fraction in the system. It was observed that gas phase diffusivity, D_{as} of toluene significantly affected the steady state aqueous phase profiles shown in Figure 13. If D_{as} was decreased by two orders of magnitude, then the concentration of toluene increased in the aqueous phase throughout the system. Similarly, decreasing D_{ao} for oxygen by two orders of magnitude resulted in decreased aerobic zones in the soil.

WASHOUT OF TOLUENE

The parameter values used for the washout study are the same as those used to simulate the steady state performance of the system (Tables 1-3). The soil-adsorption coefficient (K_{ds}) in Table 3 was calculated from Eq. (23) (Narayanan et al., 1998) with $K_{oc} = 150$ and $f_{oc} = 0.0025$. During the setup of the experimental system it was determined that the organic matter content was about 0.3% in the bottom soil of the toluene channel. However, for the simulation, organic carbon content was taken to be 0.25% at the bottom of the toluene channel. Figures 16-18 show the comparison between the modeling and experimental results during the washout of toluene following a step change in feed water from saturated toluene concentrations to pure water using 0.25% organic carbon in the simulation. Washout simulations indicated that the organic carbon content in soil has a significant impact in modeling washout of toluene from groundwater. The experimental results show that toluene concentration decreases slowly with time. This may be due to preferential flow and regions of the chamber where the fluid interchanges slowly with the bulk flow. This tailing effect does not appear to be present in the bromide data; this may be due to the short time available for bromide to enter these relatively stagnant regions. The difference may also be due to the greater tendency for toluene to adsorb to soil. The time required to remediate the chamber is somewhat longer than that predicted by the model; however, tailing is commonly observed at field sites.

Parameter sensitivity

Sensitivity analyses were also performed to study the effect of the adsorption coefficient of toluene to the soil particle surfaces. It was found that soil-adsorption coefficient appreciably affected the washout simulation of toluene. The adsorption coefficient values were varied based on the soil organic carbon content. Running the toluene washout simulation without including adsorption, by assuming the soil organic carbon content (f_{oc}) as zero, gave a significantly faster washout. When the organic carbon content was assumed to be 10-fold higher at 2.5% as compared to 0.25%, it was seen that the simulation study took a relatively longer period for washout of toluene from the channel because of more toluene adsorption onto soil.

By choosing an overall value for organic carbon content in chamber soil ($f_{oc} = 0.5\%$ g/100 g of soil), it

was observed that relatively reasonable fits were obtained between the experimental and simulated values for ports 1 and 2. However, the comparison with the data at ports 3, 4, and the outlet were then relatively poorer. Similarly, when the organic carbon content was changed to fit the washout data at ports 3, 4, and the outlet, the fit for ports 1 and 2 was relatively poorer. These difficulties may also be associated with proper modeling of the flow in the channel because of the 180° U-turn and channeling. A compromised value for organic carbon content ($f_{oc} = 0.0025$) was used for simulation.

These studies clearly indicate that soil adsorption is an important process during toluene transport through the soil. In an aquifer where soil organic matter is relatively high, significant adsorption of toluene could occur and hence influence the transport of toluene. This washout experiment was conducted after steady state concentrations of toluene should have been attained in regions of slow flow. Washout experimental data suggests that there are regions where flow is slower and that these are not well-represented in the dispersion model.

CONCLUSIONS

The simulation of phytoremediation in the experimental chamber with growing alfalfa plants and toluene provided valuable results on the effect of vegetation in the bioremediation strategy for toluene contaminated sites. Numerical and experimental results indicate that evapotranspiration associated with alfalfa plants significantly influenced the vertical movement of solutes from the saturated zone to the unsaturated zone of soil. This upward movement of water and dissolved solutes increased the availability of organic substrates to the indigenous aerobic microorganisms in the root zone of plants. Simulations indicated complete degradation of toluene in the vadose zone. Microbial growth rate, gas phase diffusivities of toluene and oxygen, and adsorption of toluene affect the fate of toluene in the chamber. The observed experimental results were in reasonable agreement with those predicted by a mathematical model which includes evapotranspiration, plant uptake, biodegradation, adsorption, oxygen transfer, and microbial growth processes. However, in the toluene washout study, the actual time required to remediate the site was considerably longer than that predicted by the model. Finally, alfalfa plants are capable of growing in laboratory conditions even when relatively high concentrations of toluene are fed continuously for long periods of time.

ACKNOWLEDGMENTS

This research was partially supported by the U.S. EPA under assistance agreements R-815709 and R-819653 to the Great Plains-Rocky Mountain Hazardous Substance Research Center for regions 7 and 8 under projects 94-12 and 94-27, and an EPA EPSCoR grant. It has not been submitted to the EPA for peer review and, therefore, may not necessarily reflect views of the agency and no official endorsement should be inferred. The U.S. Department of Energy, Office of Environmental Restoration and Waste management, Office of Technology Development and the Center for Hazardous Substance Research also provided partial funding. Students of the Fateley-Hammer group are thanked for

assistance in making FT-IR measurements. Ryan Green is thanked for assistance in the KBr study. This is contribution # 97-436-J of the Kansas Agriculture Experiment Station.

NOMENCLATURE

A	soil characteristic parameter (m)
c	soil characteristic parameter
C_k	concentration of solute k (tracer in this study) in aqueous phase (g/m^3)
d	soil characteristic parameter
D_{ak}	gas phase diffusion coefficient of solute k (m^2/hr)
D_{ij}	hydrodynamic dispersion coefficient (m^2/hr)
K_{dk}	adsorption coefficient of solute k onto soil particles (m^3/g)
K_{sat}	saturated hydraulic conductivity in soil (m/hr)
$K_{s, ij; r, ij}$	hydraulic conductivity of soil and root, respectively (m/hr)
S_e	effective saturation (m^3/m^3) (dimensionless)
t	time (hr)
V_i	convective volumetric flux in the i th direction (m/hr)
x, z	Cartesian coordinates (m) (axial and vertical directions, respectively)

Greek

α_L	dispersivity factor in the soil in the longitudinal direction (m)
α_T	dispersivity factor in the soil in the transverse direction (m)
G	lumped parameter describing the permeability of a plant's root
m_m	maximum specific growth rate for biomass (1/hr)
φ	volumetric soil-water content (m^3/m^3) (dimensionless)
$\psi_{s,r}$	soil-water and root-water pressure head (m)

Subscripts

i, j (for $i, j = x, z$)	spatial index
k	contaminant (s), biomass (b), oxygen (o), or exudates (r)

LITERATURE CITED

- Alvarez, P.J.J., P.J. Anid, and T.M. Vogel, 1994. Kinetics of Toluene Degradation by Denitrifying Aquifer Microorganisms, *J. Environ. Engrg.*, 120 (5), pp. 1327-1336.
- Anderson, T.A., E.A. Guthrie, and B.T. Walton, 1993. Bioremediation in the Rhizosphere, *Environ. Sci. Technol.*, 27, pp. 2630-2636.
- Borden, R.C., P.B. Bedient, M.D. Lee, C.H. Ward, and J.T. Wilson, 1986. Transport of Dissolved Hydrocarbons Influenced by Oxygen-limited Biodegradation 2. Field Application, *Water Resour. Res.*, 22 (13), pp. 1983-1990.
- Briggs, G.G., R.H. Bromilow, and A.A. Evans, 1982. Relationships Between Lipophilicity and Root Uptake and Translocation of Non-ionized Chemicals by Barley, *Pestic. Sci.*, 13, pp. 495-504.
- Chen, Y.M., L.M. Abriola, P.J.J. Anid, and T.M. Vogel, 1992. Modeling Transport and Biodegradation of Benzene and Toluene in Sandy Aquifer Material: Comparison with Experimental Results, *Water Resour. Res.*, 28 (7), pp. 1833-1847.
- Chiang, C.Y., J.P. Salanitro, E.Y. Chai, J.D. Colhart, and C.L. Klein, 1989. Aerobic Biodegradation of Benzene, Toluene and Xylene in a Sandy Aquifer-Data Analysis and Computer Modeling, *Ground water*, 27 (6), pp. 823-834.
- Cunningham, S.D., and W.R. Berti, 1993. Remediation of Contaminated Soils with Green Plants: An Overview, *In Vitro Cell. Dev. Biol.-Plant*, 29P, pp. 207-212.
- Davis, L.C., M.K. Banks, A.P. Schwab, M. Narayanan, L.E. Erickson, and J.C. Tracy, 1998. Plant-based Bioremediation, In: S.K. Sikdar and R.L. Irvine (Eds.), *Bioremediation: Principles and Practice*, vol. 2, Technomic Publ. Co., Lancaster, PA, pp 183-219.
- Erickson, L.E., M.K. Banks, L.C. Davis, A.P. Schwab, M. Narayanan, K. Reilley, and J.C. Tracy, 1994. Using Vegetation to Enhance In-situ Bioremediation, *Environ. Progress*, 13, pp. 226-231.
- Essaid, H.I., B.A. Bekins, E.M. Godsy, E. Warren, M.J. Baedecker, and I.M. Cozzarelli, 1995. Simulation of Aerobic and Anaerobic Biodegradation Processes at a Crude Oil Spill Site, *Water Resour. Res.*, 31 (12), pp. 3309-3327.
- Feddes, R.A., S.P. Neuman, and E. Bresler, 1975. Finite Element Analysis of Two-dimensional Flow in Soils Considering Water Uptake by Roots: II. Field Applications, *Soil Sci. Soc. Am. J.*, 39, pp. 231-237.
- Ferro, A.M., R.C. Sims, and B. Bugbee, 1994. Hycrest Crested Wheatgrass Accelerates the Degradation of Pentachlorophenol in Soil, *J. Environ. Qual.*, 23, pp. 272-279.
- Gatliff, E.G., 1994. Vegetative Remediation Process Offers Advantages Over Traditional Pump-and-treat Technologies, *Remediation*, 4 (3), pp. 343-352.
- Gibson, D.T., and Subramanian, 1984. Microbial Degradation of Aromatic Hydrocarbons, In: D.T. Gibson (Ed.), *Microbial Degradation of Organic Compounds*, Marcel Dekker, Inc., NY, pp. 181-252.
- Jin, Y., T. Streck, and W.A. Jury, 1994. Transport and Biodegradation of Toluene in Unsaturated Soil, *J. Contam. Hydrol.*, 17, pp. 111-127.
- Lee, M.D., J.M. Thomas, R.C., Borden, and P.B. Bedient, 1988. Bioremediation of Aquifers Contaminated with Organic Compounds, *Crit. Rev. Environ. Control*, 18, pp. 29-89.
- Licht, L.A., 1993. Ecolotree Cap - Densely Rooted Trees for Water Management on Landfill Covers, *Proc. Air and Waste Management Association*, 86th Annual Meeting, Paper No. 93-WA-89.07.

- Marino, M.A., and J.C. Tracy, 1988. Flow of Water Through a Root-soil Environment, *J. Irrig. and Drain. Engrg.*, ASCE, 114 (4), pp. 588-604.
- McFarlane, J.C., A. Cross, C. Frank, and R.R. Rogers, 1981. Atmospheric Benzene Depletion by Soil Microorganisms, *Env. Monit. Assess.*, 1, pp. 75-81.
- Montgomery, J.H., and L.M. Welkom, 1990. *Groundwater Chemicals Desk Reference*, Lewis Publishers, Boca Raton, FL.
- Narayanan, M., 1994. *Experimental and Modeling Studies of Bioremediation in Presence of Alfalfa Plants*, M.S. Thesis, Kansas State University, KS.
- Narayanan, M., L.C. Davis, J.C. Tracy, L.E. Erickson, and R.M. Green, 1995a. Experimental and Modeling Studies of the Fate of Organic Contaminants in the Presence of Alfalfa Plants, *J. Hazard. Mat.*, 41, pp. 229-241.
- Narayanan, M., L.C. Davis, and L.E. Erickson, 1995b. Fate of Volatile Chlorinated Organic Compounds in a Laboratory Chamber with Alfalfa Plants, *Environ. Sci. Technol.*, 29, pp. 2437-2444.
- Narayanan, M., J.C. Tracy, L.C. Davis, and L.E. Erickson, 1998. Modeling the Fate of Toluene in a Chamber with Alfalfa Plants 1. Theory and Modeling Concepts, *J. Hazard. Substance Res.*, in press.
- Perry, R.H., and C.H. Chilton (Eds.), 1984. *Chemical Engineers' Handbook*, McGraw-Hill, New York, NY, 6th ed.
- Rifai, H.S., P.B. Bedient, J.T. Wilson, K.M. Miller, and J.M. Armstrong, 1988. Biodegradation Modeling at Aviation Fuel Spill Site, *J. Irrig. and Drain. Engrg.*, ASCE, 114 (5), pp. 1007-1029.
- Schnoor, J.L., L.A. Licht, S.C. McCutcheon, N.L. Wolfe, and L.H. Carreira, 1995. Phytoremediation of Organic and Nutrient Contaminants, *Environ. Sci. Technol.*, 29, pp. 2905-2914.
- Shimp, J.F., J.C. Tracy, L.C. Davis, E. Lee, W. Huang, L.E. Erickson, and J.F. Schnoor, 1993. Beneficial Effects of Plants in the Remediation of Soil and Groundwater Contaminated with Organic Materials, *Crit. Rev. Environ. Sci. Tech.*, 23 (1), pp. 41-77.
- Stomp, A.M., H.H. Han, S. Wilbert, M.P. Gordon, and S.D. Cunningham, 1994. Genetic Strategies for Enhancing Phytoremediation, In: R.K. Bajpai and A. Prokop (eds.), *Recombinant DNA Technology II*, New York Academy of Science, NY, pp. 481-491.
- Tracy, J.C., and M.A. Marino, 1989. Solute Movement Through Root-soil Environment, *J. Irrig. and Drain. Engrg.*, ASCE, 115 (4), pp. 608-625.
- Trapp, S., and C. McFarlane (Eds.), 1995. *Plant Contamination: Modeling and Simulation of Organic Chemical Processes*, Lewis Publishers, Boca Raton, FL.
- Walton, B.T., and T.A. Anderson, 1990. Microbial Degradation of Trichloroethylene in the Rhizosphere: Potential Application of Biological Remediation of Waste Sites, *Appl. Environ. Microbiol.*, 56, pp.1012-1016.
- Winter, T.C., 1983. The Interaction of Lakes with Variably Saturated Porous Media, *Water Resour. Res.*, 19 (5), 1203-1218.
- Yaws, C.L., 1992. *Thermodynamic and Physical Property Data*, Gulf publishing company, Houston, TX.

Table 1. Soil related parameters used in the simulation study^a.

Soil Characteristic Parameters	Value
Bulk density (ρ)	1.5 g/cm ³
Saturated hydraulic conductivity (K_{sat})	0.38 m/hr
Soil characteristic parameters (A)	0.5 m
(c)	0.9
(d)	3.5
Limiting soil-water pressure head ($Y_{s, lim}$)	-12.0 m
Degree of retention (S_r)	0.15
Porosity (h)	0.35
Specific storativity (S_s)	0.00001 m ⁻¹
Specific yield (S_y)	0.20
Organic carbon content in bottom soil (f_{oc})	0.0025
Longitudinal dispersivity (α_L)	0.025 m
Transverse dispersivity (α_T)	0.001 m

^a (Marino and Tracy, 1988; Tracy and Marino, 1989)

Table 2. Plant related parameters used in the simulation study^a.

Plant Characteristic Parameters	Value
Hydraulic conductivity of alfalfa roots ($K_{r,ij}$)	0.051 m/day
Parameter for permeability of roots (G)	0.01 m ⁻¹ hr ⁻¹
Leaf area index (LAI)	5.00
Leaf area index coefficient (b)	0.875
Limiting root-water pressure head ($\gamma_{r,lim}$)	-7.0 m
Wilting root-water pressure head ($\gamma_{r,wilt}$)	-12.0 m
Root exudate loading factor (q_r)	0.0
Partition coefficient of exudates to root surfaces (R_p)	5 X 10 ⁻⁴ m ³ /m ³
Yield of biomass from exudates (Y_p)	1.0
Root density at the top ($R_{d,s}$)	0.08 m ³ /m ³
Root index drop rate (d_r)	6.0

^a(Marino and Tracy, 1988; Tracy and Marino, 1989)

Table 3. Modeling parameters used during the simulation of toluene (@ 26°C).

Microbial parameters	Value
Maximum specific growth rate (μ_m)	0.1/hr
Endogenous metabolism rate (k_{d1} ; k_{d2})	0.01/hr; 0.01 m ³ /g/hr
Partition coefficient onto root surfaces (R_b)	10.0 m ³ /m ³
Soil adsorption coefficient (K_{db})	1.0 cm ³ /g
Toluene Parameters	
Monod saturation constant (K_{rs})	50.0 mg/L
Soil adsorption coefficient (K_{ds})	0.375 cm ³ /g
Root concentration factor (R_{cf})	4.135
Transpiration stream concentration factor (T_{scf})	0.575
Yield of biomass from toluene (Y_s)	0.5 g/g
^a Dimensionless Henry's law constant (H_y)	0.274
^a Gas phase diffusivity in air (D_{as})	3.25 X 10 ⁻² m ² /hr
Oxygen Parameters	
Monod saturation constant (K_o)	0.01 mg/L
^b Dimensionless Henry's law constant (H_o)	37.5
^b Gas phase diffusivity in air (D_{ao})	7.42 X 10 ⁻² m ² /hr

^a(Montgomery and Wilkom, 1990; Yaws, 1992); ^b(Perry and Chilton, 1984)

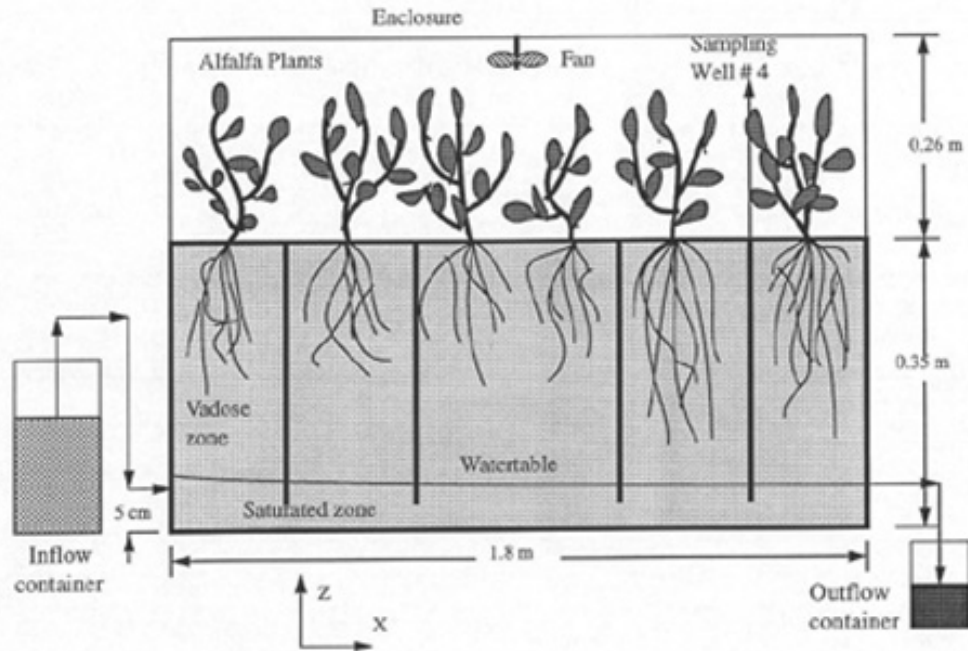


Figure 1. Schematic view of the axially extended experimental setup; the actual chamber is 0.9 m long as shown in Figure 2.

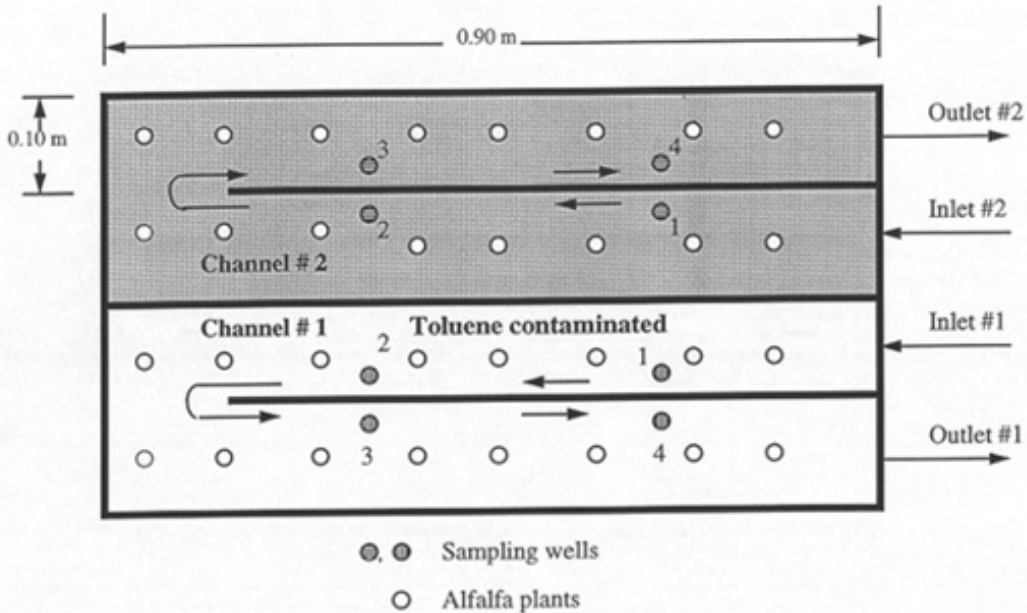


Figure 2. Overhead view of the actual experimental unit.

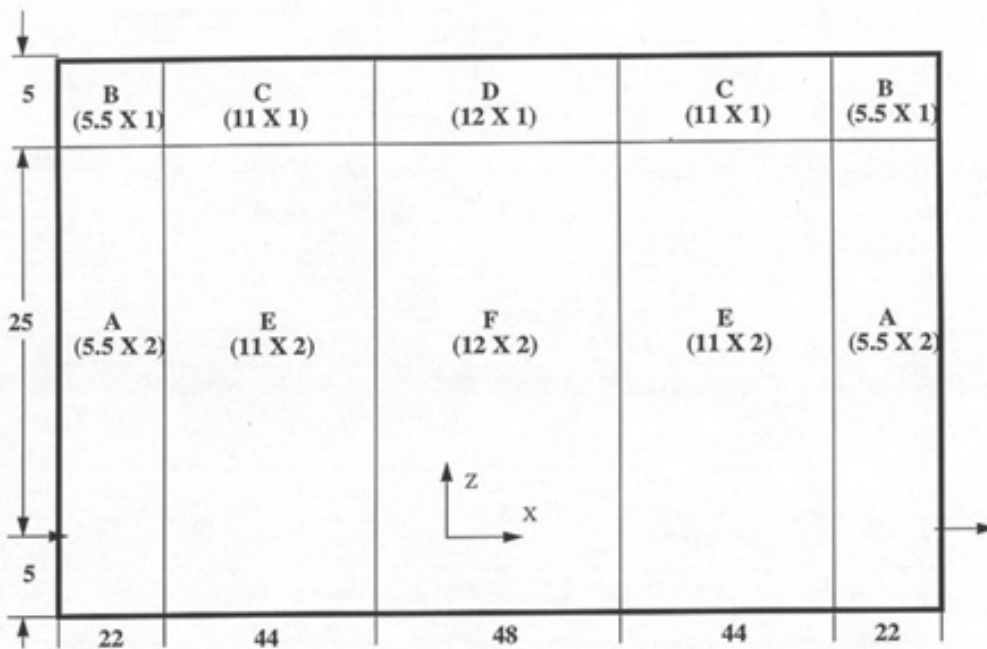


Figure 3. A schematic diagram showing the subregions with elements of identical size (shown in brackets). All dimensions are in centimeters.

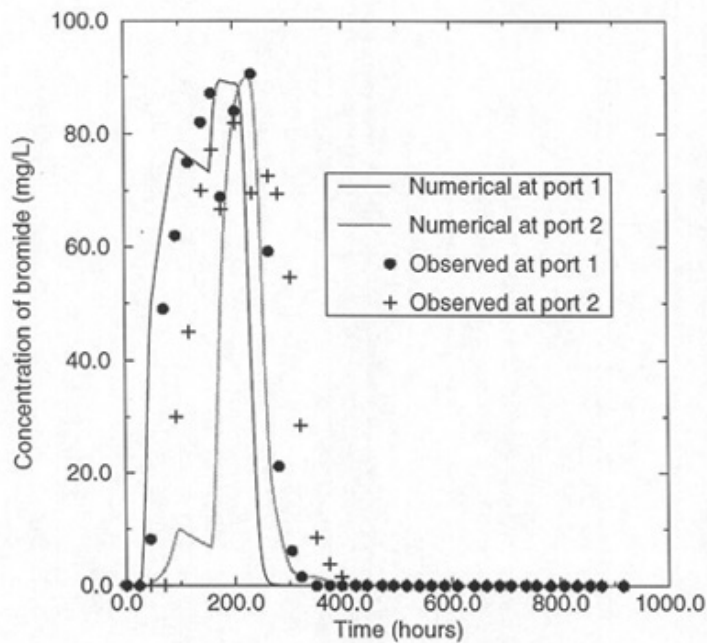


Figure 4. Comparison of simulated and experimental values for bromide tracer at port 1 and port 2.

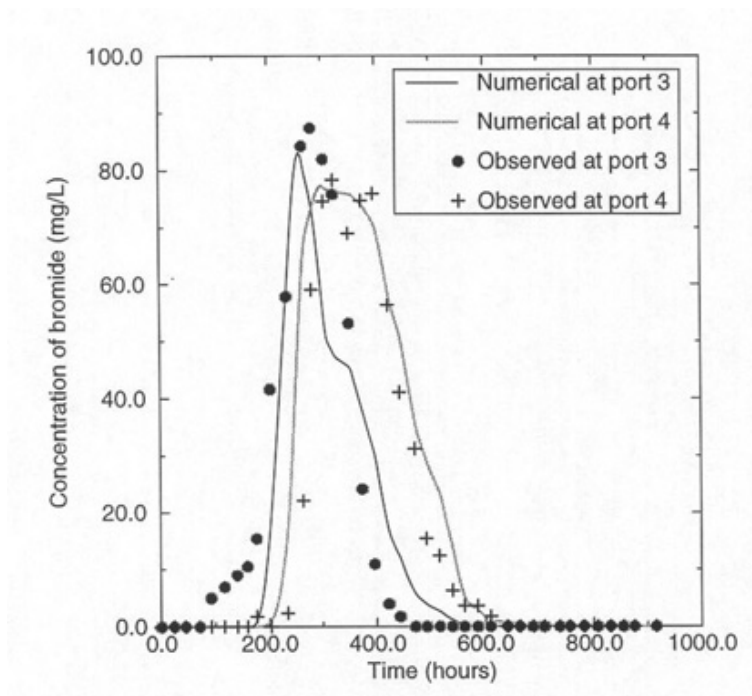


Figure 5. Comparison of simulated and experimental values for bromide tracer at port 3 and port 4.

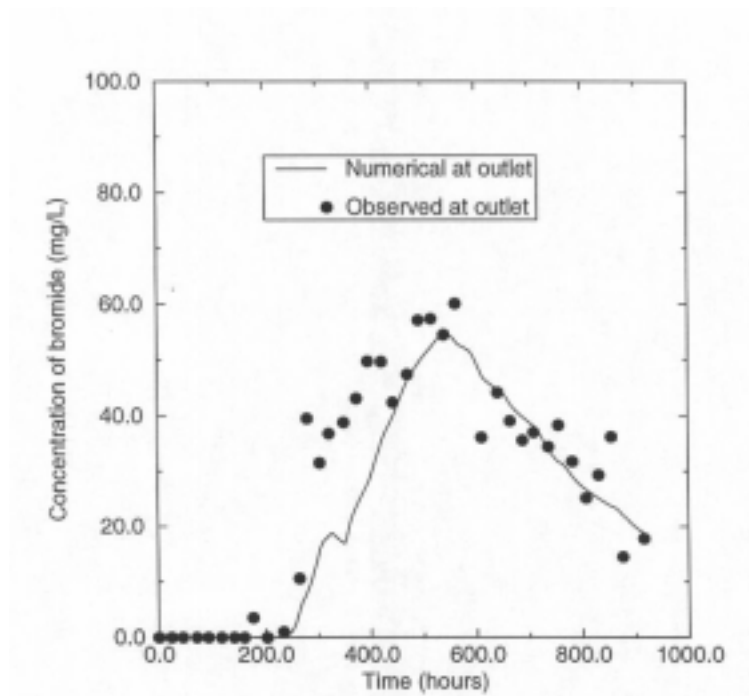


Figure 6. Comparison of simulated and experimental values for bromide tracer at the outlet.

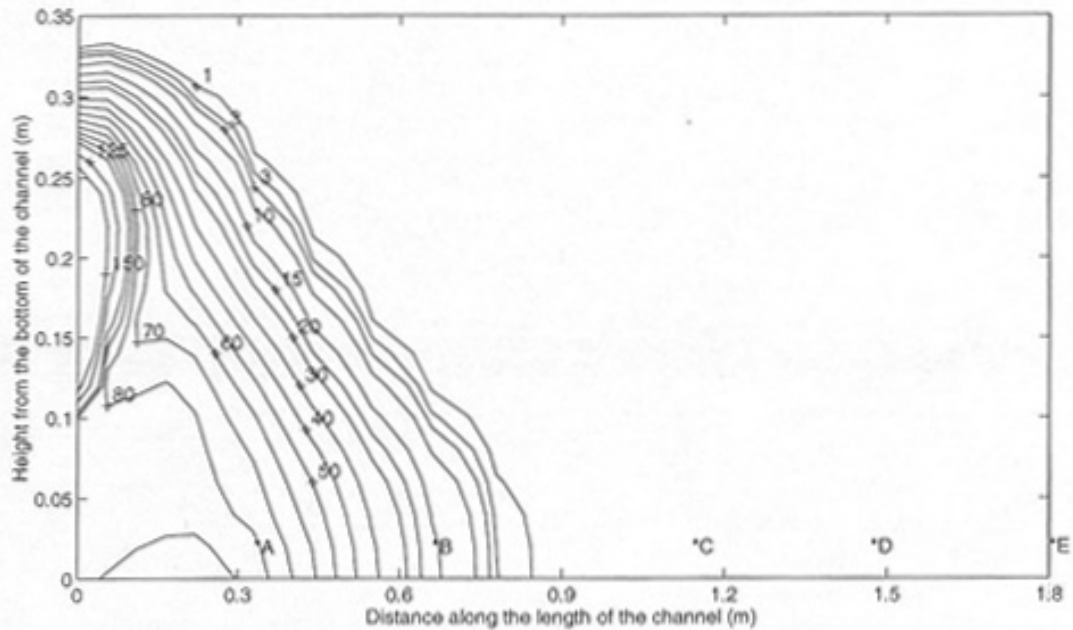


Figure 7. Simulated contour plots for bromide concentration distribution (in mg/L) in the channel after 101 hours from the start of the tracer experiment. Monitoring well concentration (in mg/L) at location A = 64; B = 17; C = D = E (outlet) = 0.

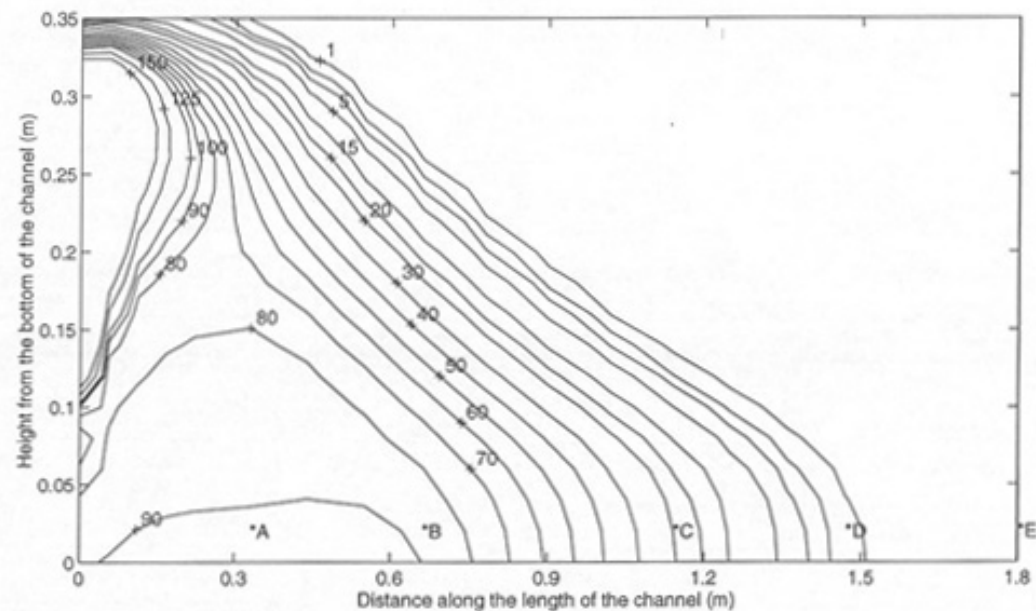


Figure 8. Simulated contour plots for bromide concentration distribution (in mg/L) in the channel after 203 hours from the start of the tracer experiment. Monitoring well concentration (in mg/L) at location A = 84; B = 82; C = 41; D = E; (outlet) = 0.

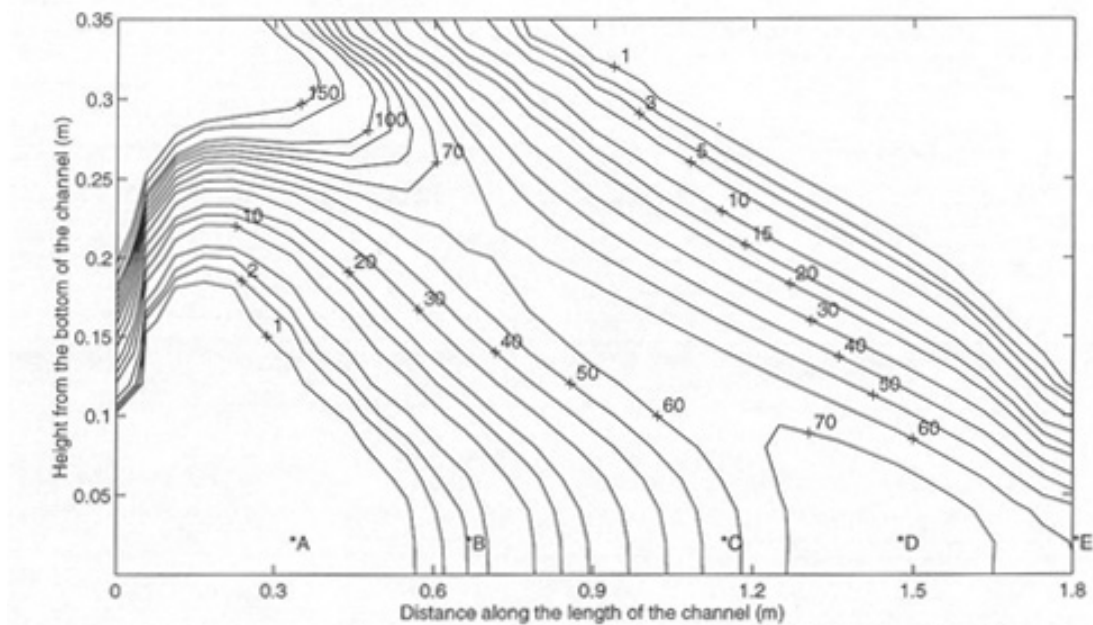


Figure 9. Simulated contour plots for bromide concentration distribution (in mg/L) in the channel after 301 hours from the start of the tracer experiment. Bromide feeding ended at 203 hours. Monitoring well concentration (in mg/L) at location A=8;B=57;C=83;D=73;E(outlet)=33.

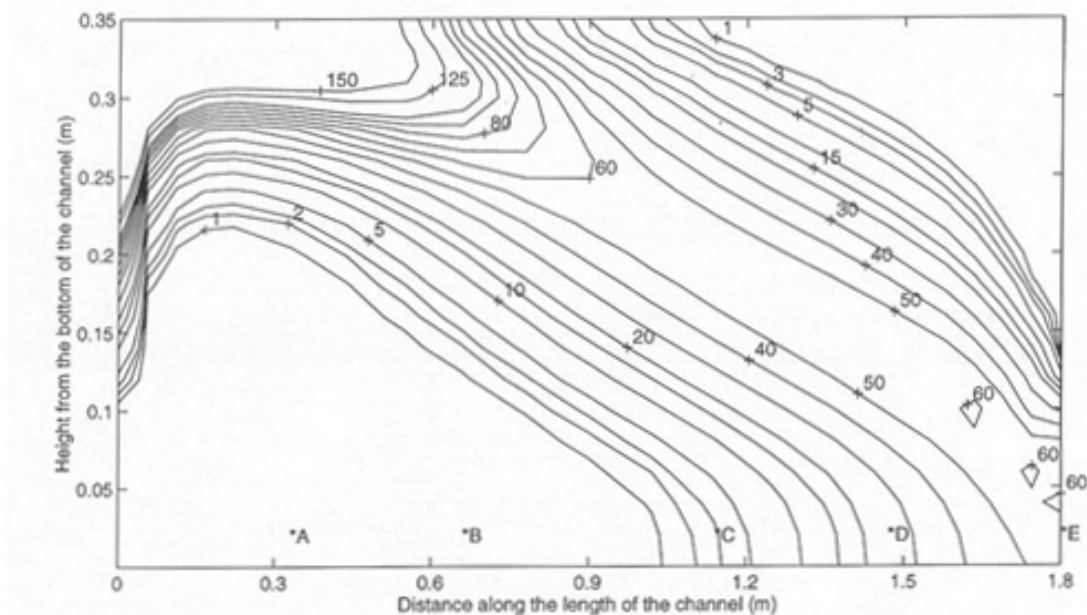


Figure 10. Simulated contour plots for bromide concentration distribution (in mg/L) in the channel after 501 hours from the start of the tracer experiment. Monitor in-well concentration (in mg/L) at location A = B = C = 0; D = 14; E (outlet) = 57.

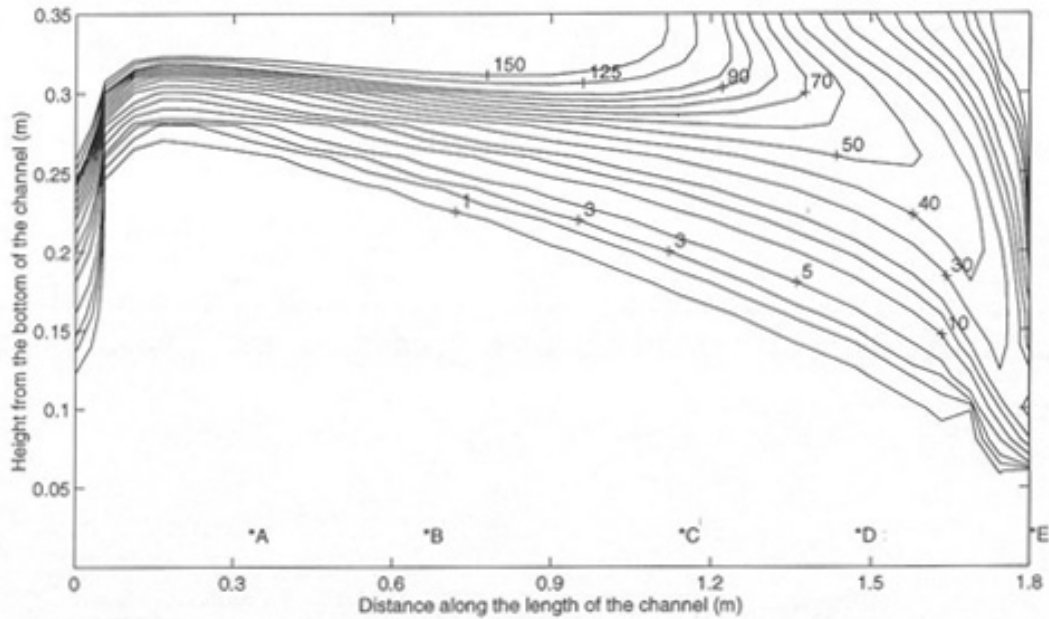


Figure 11. Simulated contour plots for bromide concentration distribution (in mg/L) in the channel after 912 hours from the start of the tracer experiment. Monitoring well concentration (in mg/L) at location A = B = C = D = 0; E (outlet) = 17.

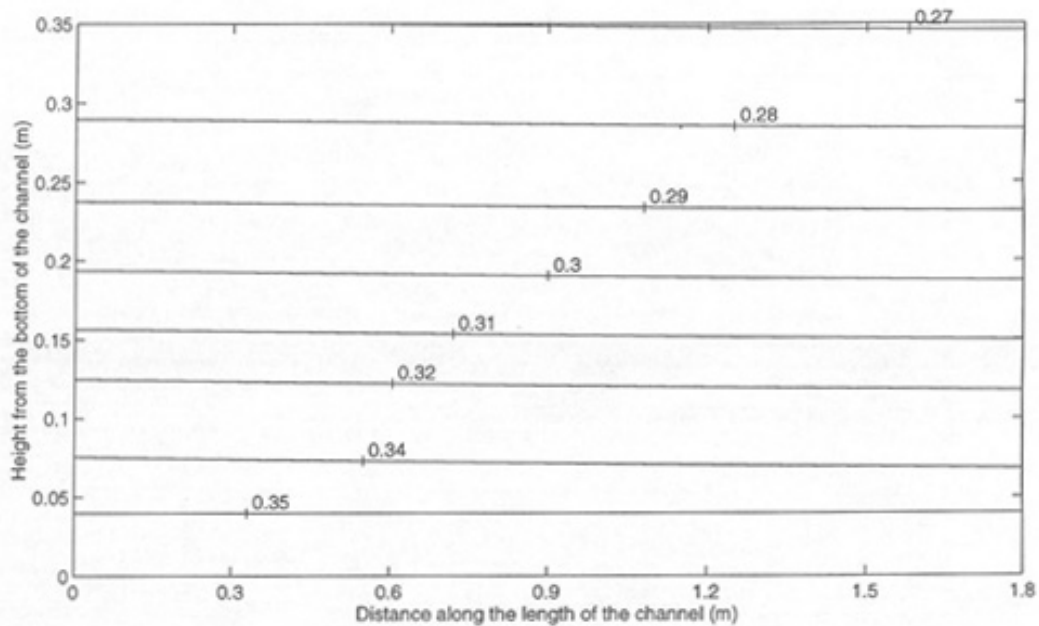


Figure 12. Simulated contour plots for water content distribution (in m^3/m^3) in the channel during steady state operation of the system. Average experimental water content values (in m^3/m^3) were 0.35 at 25-35 cm depth, 0.33 at 15-25 cm depth, and 0.27 at 5-15 cm depth, from the top.

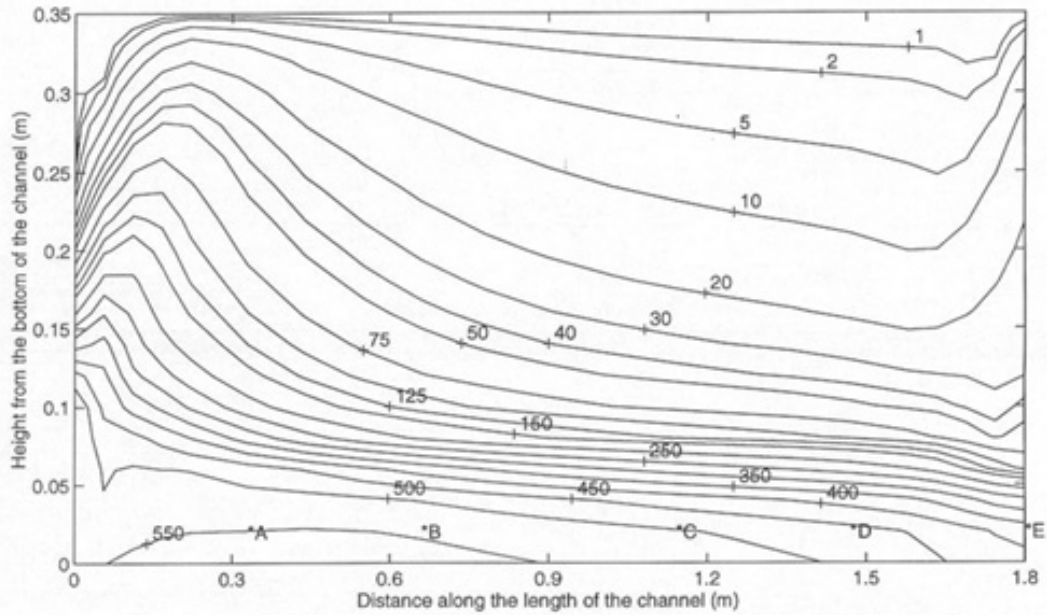


Figure 13. Simulated contour plots for toluene concentration distribution (in mg/L) in the channel during steady state operation of the system. Monitoring well concentration (in mg/L) at location A = 434; B = 418; C = 421; D = 403; E (outlet) = 455.

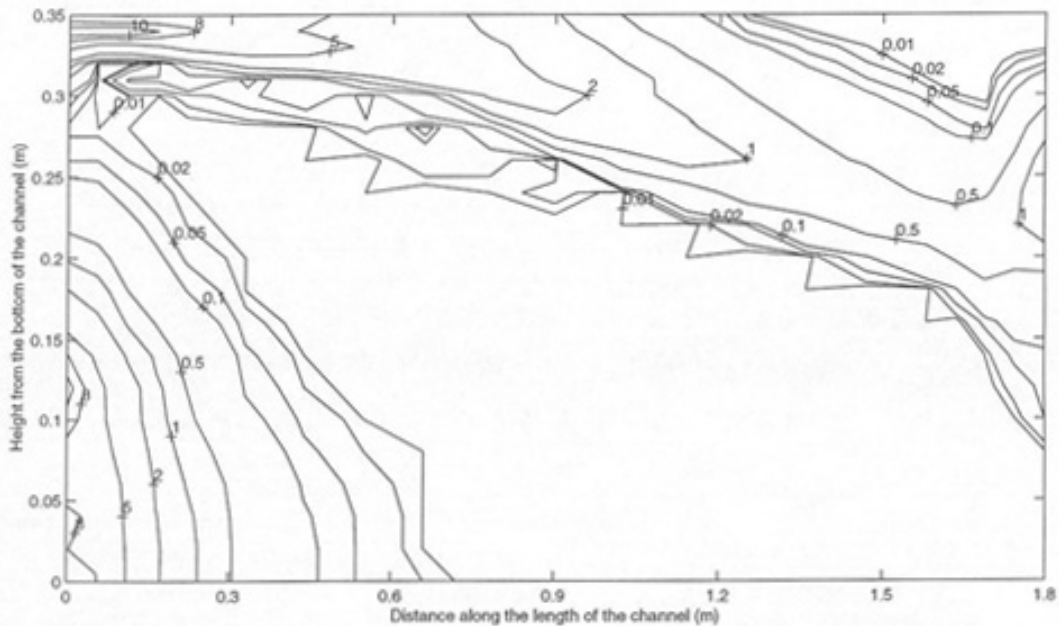


Figure 14. Simulated contour plots for biomass concentration distribution (in mg/L) in the channel during steady state operation of the system.

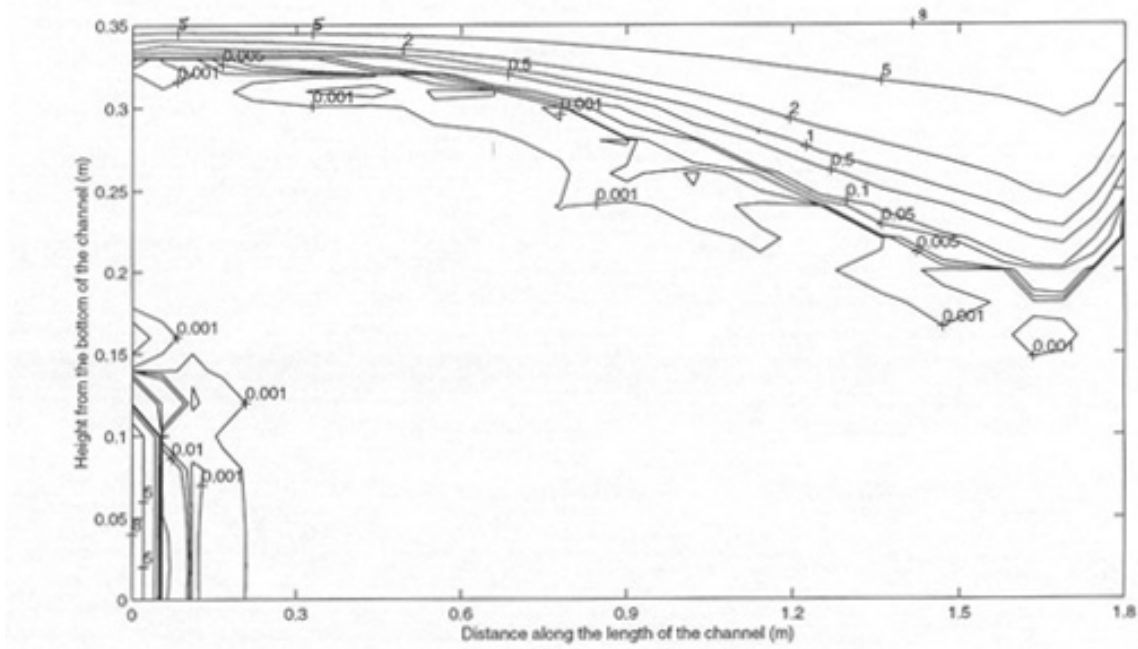


Figure 15. Simulated contour plots for oxygen concentration distribution (in mg/L) in the channel during steady state operation of the system.

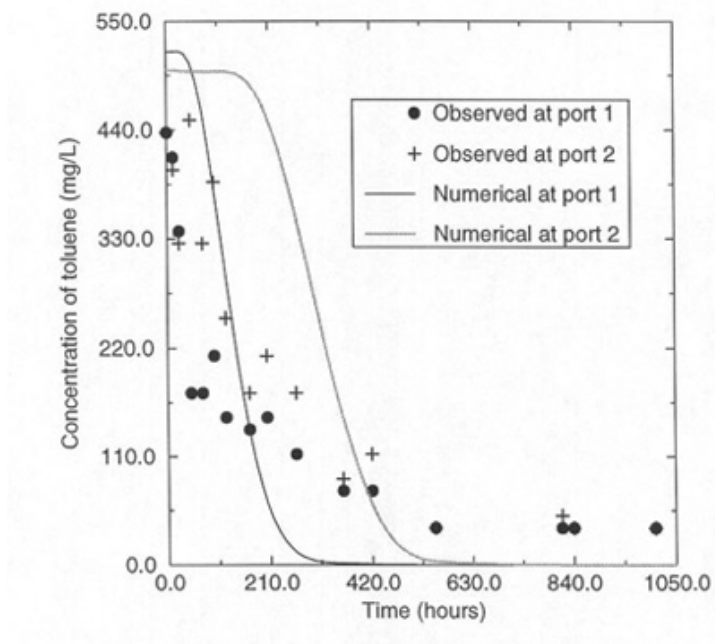


Figure 16. Comparison of simulated and experimental values during the washout of toluene at port 1 and port 2.

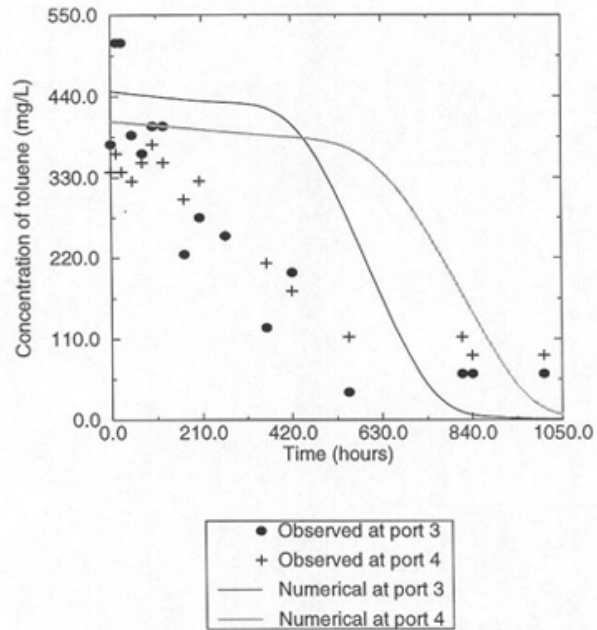


Figure 17. Comparison of simulated and experimental values during the washout of toluene at port 3 and port 4.

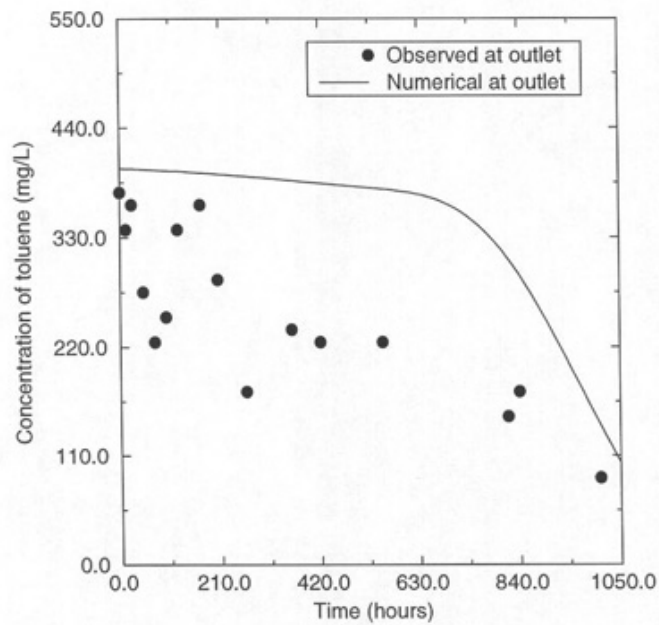


Figure 18. Comparison of simulated and experimental values during the washout of toluene at outlet.